RP Current Trends In Applied Sciences
Vol. 3, No. 1 (January – March 2024) pp. 14–19
e-ISSN: 2583-7486

RESEARCH PLATEAU PUBLISHERS

Cite this article: S. Yadav, Shreya, P. Phogat, R. Jha, S. Singh, Hydrothermal synthesis and characterization of tin telluride, *RP Cur. Tr. Appl. Sci.* **3** (2024) 14–19.

Original Research Article

Hydrothermal synthesis and characterization of tin telluride

Shikha Yadav, Shreya*, Peeyush Phogat, Ranjana Jha, Sukhvir Singh
Research Lab for Energy Systems, Department of Physics, Netaji Subhas University of Technology, New Delhi, India
*Corresponding author, E-mail: shreyasharma.aug15@gmail.com

ARTICLE HISTORY
Received: 15 Dec. 2023
Revised: 22 Jan. 2024
Accepted: 24 Jan 2024
Published online: 29 Jan. 2024

KEYWORDS
SnTe; Narrow band gap; Monochalcogenides; Hydrothermal.

ABSTRACT
Two-dimensional (2D) transition metal monochalcogenides have earned notable attention because of their distinctive electronic, physical, and chemical attributes. These materials find vast array of applications in energy generation, thermoelectric devices and gas sensing technology. Among these, tin telluride (SnTe), a member of the transition metal monochalcogenides, stands out for its remarkable qualities, featuring a narrow band gap and an environment-friendly, non-toxic nature. Prior research has demonstrated that the properties of SnTe can be effectively modified through the introduction of hydrazine during the synthesis process, resulting in enhanced conductivity and increased sensitivity to environmental changes. Consequently, SnTe has captured the interest of researchers, particularly for its gas-sensing potential. In the current study, a facile hydrothermal method was employed to synthesize SnTe and conducted an in-depth analysis of its structural,optical, and morphological characteristics through various characterization methods. The formation of SnTe with a cubic crystal structure was confirmed by X-ray diffraction (XRD) analysis, revealing a crystallite size of 67nm using the Debye Scherrer equation. Additionally, UV-Vis spectrophotometer was used to ascertain the absorbance plot and band gap of the as-synthesized SnTe sample. The hydrothermal synthesis process yielded SnTe structures with a distinctive spherical shape, as confirmed by field emission scanning electron microscopy (FESEM).

1. Introduction

Two-dimensional (2D) materials have acquired substantial attention in material research because of their exceptional gas sensing, physiochemical characteristics and their potential uses in catalysis, semiconductor devices, sensors, and biomedical applications [1]. Notably, extensive research has been conducted on graphene, the pioneering 2D material, owing to its large surface-to-volume ratio and remarkable electrical properties [2, 3]. Among the array of 2D materials, the spotlight has turned to 2D monochalcogenides, which has drawn the interest of numerous researchers due to their wide range of applications, including photovoltaics and gas sensing devices [4]. Tin telluride (SnTe) is one such material and it exists in both bulk and nano-form [5]. SnTe nanomaterials with atomic-scale thickness exhibit distinctive properties compared to their bulk counterparts. Monochalcogenides belonging to the IV-VI group (MX), where M represent elements like Sn, Ge and Pb whereas X represent elements like Se, S and Te, are known as narrow-band-gap semiconductors [4] . These non-lead containing semiconductors are well-suited for use in infrared detectors [3, 6]. SnTe, a narrow bandgap semiconductor within the IV-VI group, possesses exceptional characteristics, including high dielectric constant and an extraordinarily large value of exciton Bohr radius i.e., 95 nm and a cubic crystal structure [5]. However, pure SnTe contains intrinsic Sn vacancies, making it a thermomaterial with high thermal conductivity and low thermopower [5] . Nevertheless, SnTe is employed as a favorable p-type semiconductor in thermoelectric devices due to its environmentally friendly and non-toxic properties, offering an alternative to PbTe, which carries significant environmental risks and should be avoided [6]. SnTe emerges as a prospective thermoelectric material, offering the potential for enhanced efficiency in transforming wasted heat into valuable electrical power [7, 8]. Previous research has indicated that SnTe demonstrates high sensitivity to gases like SO_2 and Cl_2 [9]. For SnTe, several synthesis processes have been explored, such as solvothermal, vapor transport, and solution-phase approaches [4,10]. This study utilized the hydrothermal method. The synthesized sample was subjected to various characterization techniques, including FESEM, UV-Vis spectrophotometer and XRD analysis.

2. Materials and methods

2.1 Materials

$SnCl_2.2H_2O$ (Tin (IV) chloride dihydrate) and TeO_2 (Tellurium dioxide) of M/s Fisher Scientific and M/s Sigma Aldrich Pvt. Ltd. respectively, were used as precursors in the synthesis process. Hydrazine of M/s Fisher Scientific Pvt. Ltd. was also used which acts as reducing agent and ethylenediamine was used as solvent. The solutions were prepared using 15 mega-Ohm resistant DI water.

2.2 Methods

The process began by dissolving 0.105 M $SnCl_2.2H_2O$ in 40 mL DI water and 20 mL hydrazine then stirring the mixture at room temperature for 30 minutes. In a separate beaker, 0.1315 M TeO_2 was added to 40 ml DI water and 20 ml of

ethylenediamine. After continuous stirring at room temperature for 30 min, the two solutions were dissolved. This precursor mixture, with 1:1 stoichiometric ratio, was poured to teflon-lined autoclave capable of withstanding the high temperature and pressure conditions required for the hydrothermal process. The solution was prepared and added to the autoclave, which was then placed in an oven at 150˚C for 24 hours. Under these elevated temperature and pressure conditions, $SnCl_2.2H_2O$ and Te reacted with hydrated hydrazine and ethylenediamine, resulting in the formation of SnTe nanoparticles. After 24-hours reaction period, the sealed solution was then allowed to cool down. The prepared solution was centrifuged using DI water, and ethanol, then dried for 24-hours at 100˚C under vacuum conditions. Finally, the obtained sample was characterized using UV-Vis spectrophotometer, XRD and FESEM.

2.3 Characterizations

Panalytical model X'pert PRO X-ray Diffractometer was used to examine the as-synthesized samples in finely powdered form. Copper (Cu) Kα-radiation was used to obtain X- ray diffraction patterns (λ = 1.5406 A°). FESEM with an integrated EDX system (model: 761 FPlus make: JEOL) was used to analyze the morphology of the as-synthesized sample. Furthermore, a SHIMADZU UV-2600i UV-Vis spectrophotometer was employed to record the absorption spectrum.

3. Results and discussion

3.1 X-Ray diffraction

The XRD spectrum of the as-synthesized sample was analyzed at 2θ in a range of 5°to 90°. The peaks were identified and indexed in JCPDS file 98-065-2761. The observed pattern displayed a significant wide peak at 28°, suggesting a semi-amorphous characteristic. The as-synthesized sample showed a cubic crystal structure that matches with JCPDS file. Furthermore, rietveld refinement of the data was done and (h k l) values were identified as (111), (002), (022), (222), (024), and (224) at 24.56°, 28.28°, 40.33°, 50.03°, 66.24°, 73.38° respectively. The peaks of the XRD pattern are shown in Figure 1(a).

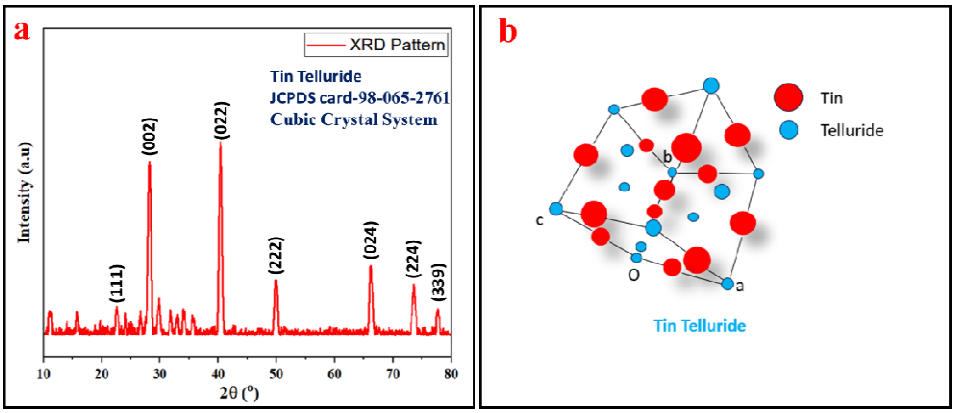

Figure 1: (a) XRD pattern for SnTe with (hkl) values on the top of the respective peak, (b) 3D structure for SnTe.

The as-synthesized SnTe has the space group Fm3m as shown in the JCPDS file. The space group "Fm3m" symbolizes a face-centered cubic crystal structure. Fm3m shows a cubic, densely packed crystal structure with a high degree of symmetry and effective atom or ion packing. Certain ionic compounds also contain Fm3m space group like cesium chloride (CsCl). It is frequently found in metallic elements, and it is known for crystallography and material research. The 3D arrangement of SnTe is shown in Fig. 1b. offers a thorough insight into the crystalline properties and structural features of the produced SnTe sample. Lattice parameter for the as-synthesized cubic structured sample was evaluated using equation (1), [12]

$$\frac{1}{d^2} = \frac{h^2}{a^2} + \frac{k^2}{b^2} + \frac{l^2}{c^2} \quad (1)$$

where, *d* means lattice spacing, (*h*, *k*, *l*) represent miller indices and *a*, *b*, *c* denotes lattice parameters. The as-synthesized sample's lattice parameters were compared to the JCPDS file in Table 1.

Table 1: Crystallographic Parameter of the as-synthesized SnTe as matched with JCPDS data.

Crystallographic Parameters	Values in JCPDS file (980652761)	Calculated values of As-synthesized SnTe
a (Å)	6.32	6.31
b (Å)	6.32	6.31
c (Å)	6.32	6.31

Table 2: Crystallite Size and Strain values of as-synthesized SnTe using W-H and S-S plot.

Method	Crystallite size (nm)	Strain
Debye-Scherrer	63	-
Williamson-Hall plot	20	0.00989
Size-Strain plot	67	0.00200

Table 3: Optical properties of as-synthesized SnTe sample.

Parameter	Value Obtained
Absorbance peaks	193.5 nm, 355.5 nm,374 nm, 417.5 nm, 471.5 nm
Band gap	0.18eV
Refractive Index	5.4
HOMO level	-2.38eV
LUMO level	-2.2eV
Absolute electronegativity	2.03

3.2 Lattice parameters, crystallite size and strain

Crystallite size is a crucial parameter for determining the presence of crystallites and learning more about preferred crystal orientations. This was calculated by the Debye-Scherrer formula given in equation (2) below, [13]

$$D = \frac{k\lambda}{\beta\cos\Theta} \quad (2)$$

where, k stands for the Scherrer constant (0.9), λ represents the wavelength (0.154 nm), Θ indicates Bragg's angle, and β corresponds to the full width at half maximum (FWHM) value. Debye-Scherrer method was based on the assumption that crystallites are defect free. Based on equation (2), it was estimated that the average size of the crystallites is around 63 nm. Smaller crystallite sizes typically yield a greater surface area per unit volume, influencing the material's reactivity and proving beneficial in applications such as catalysis or sensing. To obtain more accurate value of strain as well as the crystallite size, Williamson Hall (W-H) plot was employed, W-H Plot was plotted to get an estimate of the strain and confirm the crystallite size. The formula used for this is equation (3), [11]

$$\beta\cos\Theta = 4\varepsilon\sin\Theta + \frac{k\lambda}{D} \quad (3)$$

where β (in radian) is FWHM of obtained peak, Θ (in radians) is Bragg's angle of corresponding peak, ε represent crystallite strain in the sample, D is crystallite size and k (Scherrer constant) has 0.9 value. The linear fitted graph is plotted between βcos Θ on y axis and 4sinΘ on x-axis which is known W-H plot depicted in Figure 2(a).

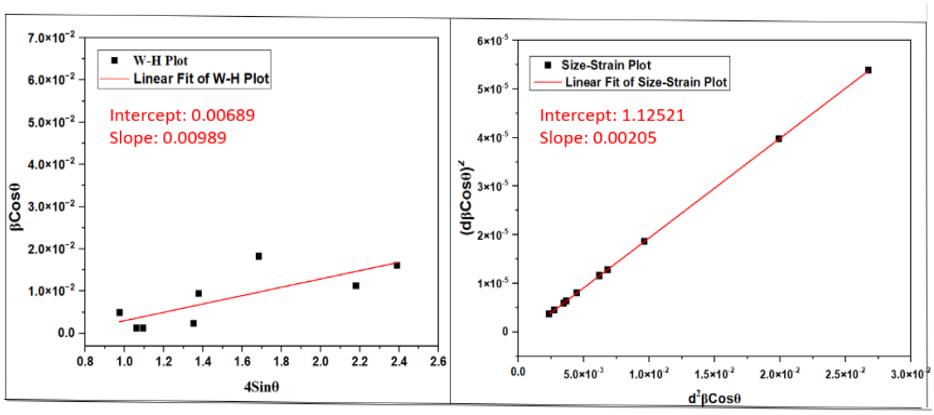

Figure 2: (a) W-H plot (b) Size Strain plot.

The equation (3) was compared to the standard linear equation $y = m(x) + c$. The strain in the sample was derived from the slope of graph while the intercept was used to find the crystallite size using relation (4), [12]

$$\frac{k\lambda}{\text{Intercept}} = D \quad (4)$$

The average lattice strain was put equal to slope i.e., 0.00989. The crystallite size was evaluated and was noted to be 20 nm. Furthermore, the crystallite size and lattice strain were also computed using the Size-Strain plot method. The size-strain plot is used for a wide range of materials, including those with smaller crystallites and intrinsic microstructure. It offers a more accurate and direct way to get microstrain. In this method size and strain were calculated using equation (5), [7]

$$(d\beta\cos\Theta)^2 = \frac{k\lambda}{D}(d^2\beta\cos\Theta) + \frac{\varepsilon^2}{4} \quad (5)$$

The crystallite size calculated using equation (5) is 67 nm and the size strain was found to be 0.002. The results are found to be in accordance with the crystallite size determined using the Debye Scherrer equation. The graph was plotted with the diffraction peaks ($d^2_{hkl}\times \beta_{hkl}\times \text{Cos}\Theta$) on the x-axis and $(d_{hkl}\times\beta_{hkl}\times \text{Cos}\ \Theta)^2$ on the y-axis and the graph of the size strain plot is depicted in Figure 2(b).The concentration of defects present per unit volume is referred to as dislocation density. The dislocation density of the as-synthesized sample is proportional to the strain and inversely related to the crystallite size. It is mathematically given by equation (6), [13]

$$\text{Dislocation Density } (\delta) = \frac{1}{D^2} \quad (6)$$

The dislocation density values determined using equation (6) is given as 2.1754×10^{-4}.

3.3 UV-Vis spectroscopy

The prepared sample was examined using a UV-Vis spectrophotometer to determine absorbance plot and optical

bandgap. The optical characteristics of the preparedsample were examined in the range of 190 nm to 850 nm. The graph showed several absorbance peaks, with the significant absorbance found in the visible region. The absorption peaks depicted in Fig. 3a are 193.5, 355.5, 374, 417.5, and 471.5 nm. The absorbance curve showedbroad absorption peaks in the visible range.The absorbance data obtained was used to find various properties of the sample, such as the refractive index, optical bandgap, conduction, and valence bandgap. Based on the absorbance data, the Tauc plot was generated using Beer-Lambert's lawto determine the optical bandgap of the prepared sample by linear fitting the selected data as shown in Fig. 3b as, [14]

$$\alpha h\nu = A[h\nu - E_g]^{1/n} \quad (7)$$

where, a denotes absorbance in arbitrary units (a.u.); α signifies the molecular extinction coefficient; h is Planck's constant, and ν is the frequency (ν = λ/c) calculated as the ratio of wavelength (λ) to the speed of light (c). In the band gap, the parameter n takes on values of ½ for a direct band gap and 2 for an indirect band gap. At room temperature, the standard bandgap value for SnTe is 0.18 eV, precisely matching the value determined using the Tauc plot equation (7) for the as-synthesized sample, as depicted in Figure 3(b).This characteristic makes it a narrow band gap semiconductor suitable for thermoelectric and gas sensing application.

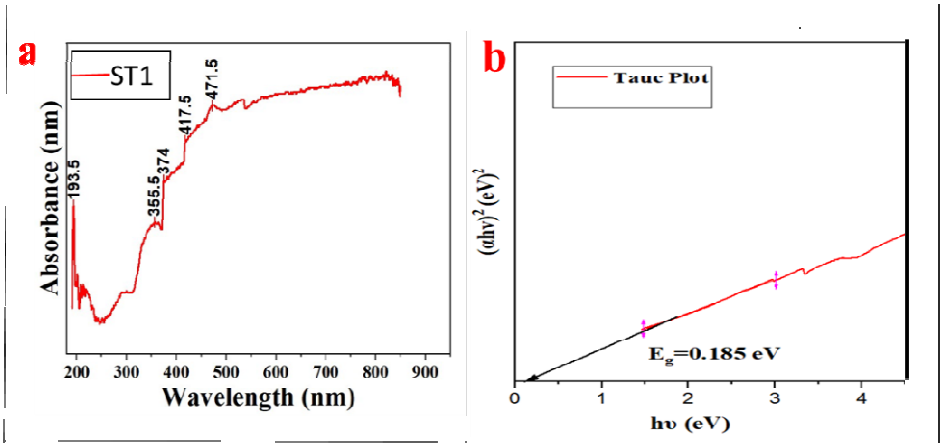

Figure 3: (a) UV-Vis absorbance spectrum for as-synthesized samples and (b) Tauc plot for as-synthesized sample.

3.4 Refractive index

It is the fundamental property for analyzing the interaction of light with the sample and understanding its behavior. The optical properties of a material, particularly the phase velocity of light within the sample, are greatly influenced by the refractive index, which plays a crucial role in determining these characteristics. The value of refractive index of the synthesized SnTe was determined by putting the value of the energy band gap in the below-mentioned equation (8), [5, 7]

$$\frac{n^2-1}{n^2+2} = 1 - \sqrt{\frac{E_g}{20}} \quad (8)$$

where, n represent refractive index; E_g is energy band gap. Using equation (8), the evaluated value for the refractive index is 5.4.

3.5 Conduction and valence band

The positions of valence band and conduction band were determined using the equation (9) and (10) provided below, [12, 15]

$$E_{VB} = \square - E_e + 0.5\, E_g \quad (9)$$

$$E_{CB} = E_{VB} + E_g \quad (10)$$

Here, □ is absolute electronegativity and E_e stands for free electron energy.

The absolute electronegativity for SnTe is 2.03. On putting this value in the equation (9), the obtained value of valence band is -2.38 eV. Also, the value of Conduction band is -2.2 eV which was determined by putting this value in equation (10).

3.6 Field emission scanning electron microscopy (FESEM)

The surface characteristics of the as-synthesized samplewere determined using FESEM images and an EDX spectrum. The morphology of the sample was depicted using FESEM, revealing a spherical-shaped structure as shown in Fig. 4(a) & 4(b). The images depicts the formation of nano-spheres of varying sizes. These images were captured at different areas with an appropriate magnification scale, ranging from 100 nm to 1 µm. An EDS spectrum was used to study the elemental composition of prepared sample in this area. The EDS spectrum of the corresponding sample area confirmed the presence of SnTe through the identification of intensity peaks for Sn and Te elements.

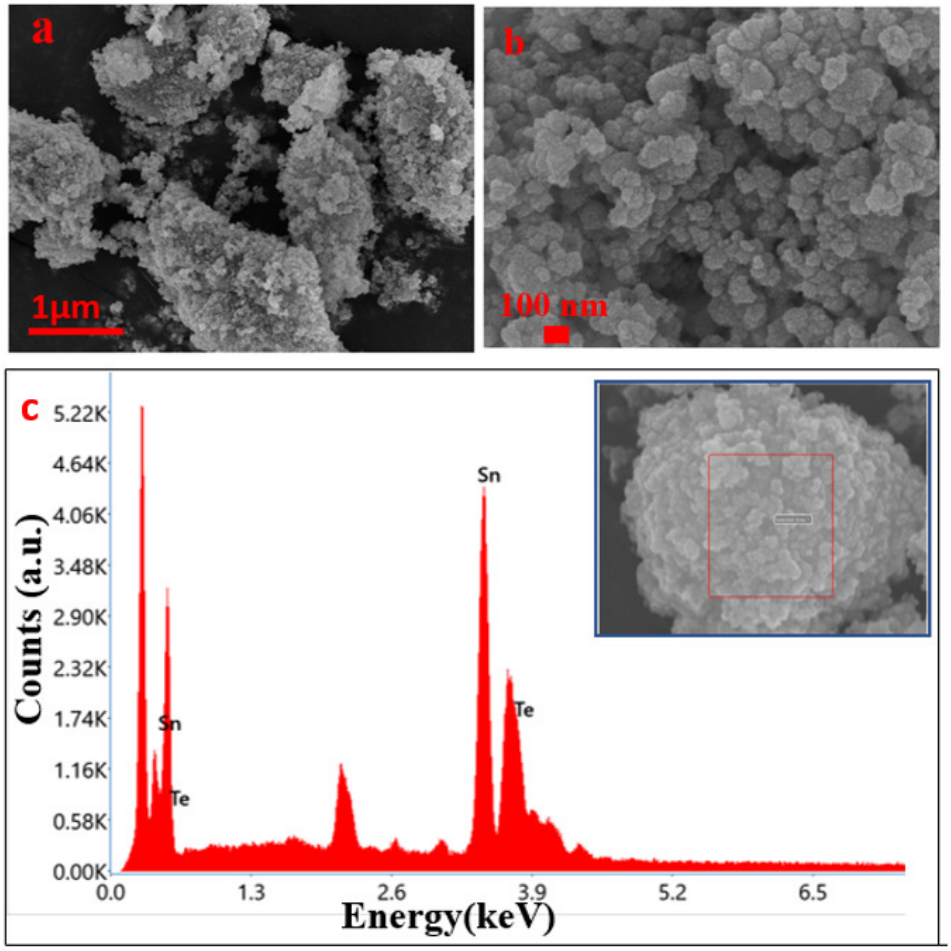

Figure 4: (a, b) Shows FESEM images of as-synthesized sample; (c) EDS pattern of the corresponding selected area of SnTe.

4. Conclusions

In this study, non-toxic precursors and solvents, such as $SnCl_2 \cdot 2H_2O$, TeO_2, hydrazine, and ethylenediamine, were employed. Using these chemicals, SnTe was successfully synthesized through a straightforward and cost-effective hydrothermal method. In this work, SnTe having a direct and narrow band gap (0.18eV) was synthesized, which has potential applications in fields such as infrared detection, thermoelectric materials, and gas sensing devices. This technique provides a fundamental approach to manufacturing SnTe semiconductors. Tin telluride, as a group IV-VI semiconductor, holds significant promise for future research.

Acknowledgements

The authors gratefully acknowledge essential resources provided by Prof. Ashok Kumar Nagawat, Vice Chancellor of Netaji Subhas University of Technology (former Netaji Subhas Institute of Technology, University of Delhi).

Author contributions

Shikha Yadav: Conceptualization, Writing - original draft and Formal analysis. Shreya and Peeyush: Formal analysis and software. Ranjana Jha: Supervision. Sukhvir Singh: Writing - review and editing.

References

[1] I.S. Raja, M. Vedhanayagam, D.R. Preeth, C. Kim, J.H. Lee, D.W. Han, Development of two-dimensional nanomaterials based electrochemical biosensors on enhancing the analysis of food toxicants, *Int. J. Mol. Sci*. **22** (2021) 3277.

[2] P. Phogat, Shreya, R. Jha, S.Singh, Electrochemical analysis of thermally treated two dimensional zinc sulphide hexagonal nano-sheets with reduced band gap, *Phys. Scr*. **98** (2023) 125962.

[3] L. Ge, X. Mu, G. Tian, Q. Huang, J. Ahmed, Z. Hu, Current applications of gas sensor based on 2-D nanomaterial: A mini review, *Front. Chem*.**7** (2019) 839.

[4] D. Feng, Z.H. Ge, Y.X. Chen, J. Li, J. He, Hydrothermal synthesis of SnQ (Q = Te, Se, S) and their thermoelectric properties, *J. Nanotechnol*. **28** (2017) 455707.

[5] R.M. Kannaujiya, A.J. Khimani, S.H. Chaki, Growth and characterizations of tin telluride (SnTe) single crystals, *Eur. Phys. J. Plus* **135** (2020) 1.

[6] R. Moshwan, L. Yang, J. Zou, Z.G. Chen, Eco-friendly SnTe thermoelectric materials: progress and future challenges, *Adv. Funct. Mater*. **27** (2017) 1703278.

[7] T. Kumar, P. Phogat, V. Sahgal, R. Jha, Surfactant-mediated modulation of morphology and charge transfer dynamics in tungsten oxide nanoparticles, *Phys. Scr*. **98** (2023) 085936.

[8] W. Chen, Q. Zhou, F. Wan, T. Gao, Gas sensing properties and mechanism of nano-SnO_2-based sensor for hydrogen and carbon monoxide, *J. Nanotechnol*. **2012** (2012) 1.

[9] G. Wei, J. Pang, J. Zhang, H. Chen, K. Wang, J. Yan, S. Wei, Mn-doped SnTe monolayer as toxic gas scavenger or sensor based on first-principles study, *Phys. Scr*. **98** (2023) 075941.
[10] M. Salavati-Niasari, M. Bazarganipour, F. Davar, A.A. Fazl, Simple routes to synthesis and characterization of nanosized tin telluride compounds, *Appl. Surf. Sci*. **257** (2010) 781-785
[11] Shreya, P. Phogat, R. Jha, S. Singh, Microwave-synthesized γ-WO_3 nanorods exhibiting high current density and diffusion characteristics, *Transit. Met. Chem*. **48** (2023) 167-183
[12] P. Phogat, Shreya, R. Jha, S. Singh, Optical and microstructural study of wide band gap ZnO@ZnS core–shell nanorods to be used as solar cell applications, in: *Recent Advances in Mechanical Engineering*, B.Sethuraman, P.Jain, M. Gupta (Eds.), Springer Nature, Singapore (2023) pp. 419-429.
[13] P. Phogat, D. Kumari, S.Singh, Fabrication of tunable band gap carbon based zinc nanocomposites for enhanced capacitive behaviour, *Phys. Scr*. **98** (2023) 095030.
[14] S. Sharma, P. Phogat, R. Jha, S. Singh, Electrochemical and optical properties of microwave assisted MoS_2 nanospheres for solar cell application, *Int. J. Smart Grid Clean Energy* **12** (2023) 66-72.
[15] U.S. Shenoy, D.K. Bhat, Molybdenum as a versatile dopant in SnTe: a promising material for thermoelectric application, *Energy Adv*. **1** (2022) 9-14